Final Report

INVESTIGATION OF SPACE STABLE

THERMAL CONTROL COATING

PROPERTIES

October 1971

TELEDYNE
BROWN ENGINEERING

Research Park • Huntsville, Alabama 35807

FINAL REPORT
SE-SSL-1410

INVESTIGATION OF SPACE STABLE
THERMAL CONTROL COATING PROPERTIES

By

T. Mookherji

October 1971

Prepared For

SPACE SCIENCES LABORATORY
GEORGE C. MARSHALL SPACE FLIGHT CENTER
HUNTSVILLE, ALABAMA

Contract No. NAS8-25900

Prepared By

SCIENCE AND ENGINEERING
TELEDYNE BROWN ENGINEERING
HUNTSVILLE, ALABAMA

ABSTRACT

A capability to study the nuclear magnetic resonance of space-craft thermal control coating has been built utilizing an Alpha Scientific electromagnet and Varian Associates V-series and WL-series electronics. The electronics associated with the electromagnet had to be modified to make it compatible with the resonance measuring system. Resonance measurements have been performed on ZnO, Zn_2TiO_4 and FEP Teflon. The failure to observe resonance in ZnO and Zn_2TiO_4 has been theoretically explained. The linewidth and second moment measurements on ultraviolet irradiated FEP Teflon shows that there is no measurable degradation of the material due to short term irradiation.

APPROVED:

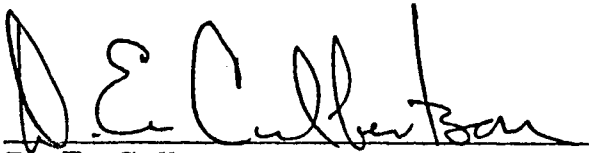N. E. Chatterton, Ph.D.
Manager
Research Engineering Department

D. E. Culbertson
Vice President

TABLE OF CONTENTS

LIST OF ILLUSTRATIONS

INTRODUCTION

One of the many important facets of the complex problem of space flight is that of environmental control of the space vehicle. The control of spacecraft temperature is usually accomplished by passive methods, generally by the selection of appropriate surfaces and coatings to provide optimum reflectance, absorptance, and emittance of solar and infrared radiation. A major problem encountered with the thermal control coatings now in use is the severe change in the solar absorptance to thermal emittance ratio (α_s/ϵ_{IR}) of the coatings as a result of solar ultraviolet radiation and charged particle bombardment. This change causes an increase in the temperature of the interior of the spacecraft, degrading the performance of the equipment aboard. Such changes have caused the complete failure of some deep space probes. These failures led to the establishment of a program aimed at developing more space-stable thermal control coatings.

For several years, research has been directed toward the development of a model which adequately describes the degradation mechanism. These studies have demonstrated two general effects of the radiation on white oxide-based paint coatings which result in an increase in the (α_s/ϵ_{IR}) ratio. Proton irradiation generally causes a large increase in the absorption coefficient for the visible spectral region, while electron irradiation and/or ultraviolet irradiation cause a large increase in the absorption coefficient for the near infrared spectral region and a much smaller increase in the absorption coefficient for the visible spectral region. Since the development of a basic physical model for the degradation process is necessary to the systematic development of space-stable thermal control coatings, studies were concentrated on the most promising candidate materials. Because of

1

its success on short-term space flights, ZnO was chosen as the prime study material to be used in developing a degradation model. However, the studies to date have not been definitive enough to exactly and uniquely describe the degradation process.

One of the theories advanced for ZnO indicates that the damage is a result of oxygen from the surface of the particles being liberated through radiation-induced holes (Ref. 1). This loss of oxygen results in the presence of oxygen vacancies and excess zinc content in the sample. It is postulated that the oxygen vacancies thus created trap electrons when the Fermi level is above these states and that the excitation of these electrons to the conduction band provides the infrared absorption. Although the mechanism for the visible absorption is still rather vague, it has been postulated that this damage is the result of the excess surface zinc diffusing into the particle and causing lattice strain. However, other models can also describe the damage. For example, the irradiation can produce excess zinc which acts as donor centers. When these centers are filled with electrons, they become sensitive to infrared radiation (Ref. 2). F-center production may be responsible for the increased visible absorption (Ref. 3). The damaging radiation may interact with impurities in the material to produce the absorption centers.

In addition to paints, the requirement for low α_s to ϵ ratio can be achieved with a transparent coating over good solar reflectors. These reflectors are known as Optical Solar Reflectors (OSRs). The most promising form of OSRs which NASA is currently considering consists of vacuum-deposited aluminum or silver over a thin FEP Teflon sheet. These OSRs are placed on the spacecraft such that the Teflon "sees" the Sun and space.

Polymers are known to undergo degradation because of thermal, ultraviolet, and charged particle radiation. FEP Teflon degrades when exposed to thermal and high-energy radiation, with a resultant adverse effect upon the physical properties. Besides degradation in other physical properties, such as melt viscosity, color, tensile strength, etc., Teflon yields monomers and fluorine because of chain scission caused by thermal, untraviolet, and charged particle radiation. Once this chain scission is initiated, it proceeds to unzip (chain reaction) rapidly into monomers until the entire chain is consumed.

Since ultraviolet is a major component of space radiation, a better understanding of the ultraviolet irradiation degradation mechanism is necessary to provide a basis for developing a suitable thermal control coating for spacecraft exterior surfaces. To gain this understanding of the degradation mechanism, experiments were conducted to investigate the nuclear magnetic resonance (NMR) of zinc oxide powder and FEP Teflon in the form of thin sheet.

EXPERIMENTAL APPROACH

THEORETICAL BACKGROUND

Many atomic nuclei in their ground state have a non-zero spin angular momentum $I\hbar$ and a dipolar magnetic moment $\mu = \gamma\hbar I$ collinear with it, where γ is the magnetogyric ratio for the nucleus. With few exceptions, the order of magnitude of these moments is between 10^{-3} and 10^{-4} Bohr magnetons. It is these moments that give rise to nuclear magnetism. The existence of relaxation phenomena has great importance in the study of nuclear magnetism. It is because of the relaxation mechanisms that the nuclear spins can "feel" the temperature of the lattice, and that differences of populations can appear between the various energy levels of the nuclear spin system, leading to a net absorption by the spin system of r.f. power supplied by an external generator. It is a consequence of these differences that a net nuclear magnetization

$$M = X_o H_o = \frac{N\gamma^2 \hbar^2 I(I+1) H_o}{3kT}$$

of N spins, appears in an applied field H_o.

The conditions under which a nuclear magnetic resonance is observed are manifold. A distinction can be drawn between the use of very small r.f. fields which can be assumed to leave the populations of the spin states practically unperturbed, and that of large r.f. fields which appreciably decrease the differences between the populations of the spin states -- a phenomenon known as saturation. Another distinction can be made between so-called slow-passage methods where at each stage of the experiment a quasi-state is reached, and transient

methods where non-equilibrium situations occur. Material properties produce differences between the behavior of solid samples and fluid samples. In the solids there is usually a tight coupling between the nuclear spins which considerably complicates the phenomenon of nuclear resonance. In fluids this coupling is quenched to a considerable extent by the rapid relative motions of the spins.

The amount of r.f. energy absorbed per unit time by a sample containing N spins per unit volume of magnetic moment $\gamma \hbar I$ is computed using the formula

$$W_m (m - 1) = \frac{2\pi}{\hbar} \frac{\gamma^2 \hbar^2}{4} H_1^2 \mid (m|I_+|m-1) \mid^2 \frac{g(\nu)}{h}$$

$$= \tfrac{1}{4} \omega_1^2 (I + m) (I - m + 1) g(\nu)$$

which gives the transition probability per unit time induced by a rotating r.f. field of frequency $\omega = 2\pi\nu$ and amplitude $H_1 = \omega_1 /\gamma$.

If the assumption of negligible saturation can be made, the difference in populations between the states $I_z = m$ and $I_z = (m - 1)$ is, for each spin

$$P_{m-1} - P_m = P_m \left[\exp \left(\frac{\hbar\omega_0}{kT}\right) - 1\right] \cong \frac{1}{(2I + 1)} \frac{\hbar\omega_0}{kT} \quad .$$

The total energy absorbed per unit time will thus be

$$P = \hbar\omega \frac{\hbar\omega_0}{kT} \frac{1}{(2I + 1)} \frac{\pi\omega_1^2}{2} \sum_{m=I}^{I+1} \mid (m|I_+|m-1) \mid^2 N f(\omega)$$

$$= \frac{\hbar^2 \omega\omega_0}{kT} \frac{\gamma^2 H_1^2}{6} I (I + 1) 2\pi N f(\omega) \quad .$$

5

The origin of the finite width of spin levels described by the shape function $f(\omega)$ may be caused by dipolar interactions between the spins, by the inhomogeneity of the applied field, by fluctuating local magnetic fields, etc.

The rate of absorption is proportional to the imaginary component of the nuclear magnetic susceptibility

$$\chi = \chi' - i\chi'' \ .$$

The r.f. power absorbed by the spin system will then be given by

$$P = 2H_1^2 \ \chi'' \ \omega \ .$$

This in terms of χ'_0 will be

$$\chi''(\omega) = \tfrac{1}{2}\pi \ \chi_0 \omega_0 \ f(\omega) \ .$$

The shape function $f(\omega)$ will in general be a bell-shaped narrow curve with a maximum at the Larmor frequency ω_0 of the spin system and, since $f(\omega)$ is normalized to unity, it will have a width Δ such that $\Delta f(\omega_0) \sim 1$.

Considerable insight into the macroscopic aspects of the nuclear magnetic resonance method can be gained by an examination of the Bloch equations. The complete solution of these equations is difficult and usually need not be considered since the essential features of magnetic resonance absorption can be illustrated by a steady state solution. That is, H_0 and H_1 fields are considered to have been applied for a sufficient period of time that the z-component of the total

magnetization M_z is constant, and the other two components M_x and M_y rotate with the H_1 field. The steady state solution is obtained by a transformation to a set of coordinates which rotates with H_1 field. M_z will be unaffected, but M_x and M_y must be redefined in terms of the rotating frame. u is defined to be the component of (M_x, M_y) which is in phase with the H_1 field and v is the perpendicular component which is out of phase. The transformation equations can be expressed as

$$
\begin{pmatrix} M_x \\ M_y \end{pmatrix} = \begin{pmatrix} \cos \omega t & - \sin \omega t \\ - \sin \omega t & - \cos \omega t \end{pmatrix} \begin{pmatrix} u \\ v \end{pmatrix} .
$$

In terms of this transformed coordinate system, the steady state Block equations yield

$$
M_x = \frac{T_2^2 (\omega_0 - \omega) \gamma H_1}{1 + T_2^2 (\omega_0 - \omega)^2 + \gamma^2 H_1^2 T_1 T_2} M_0
$$

$$
My = \frac{\gamma H_1 T_2}{1 + T_2^2 (\omega_0 - \omega)^2 + \gamma^2 H_1^2 T_1 T_2} M_0
$$

$$
M_z = \frac{1 + T_2^2 (\omega_0 - \omega)^2}{1 + T_2^2 (\omega_0 - \omega)^2 + \gamma^2 H_1^2 T_1 T_2} M_0 .
$$

The component rotating in the same direction as the Larmar precession of the magnetization vector is of the same sign as ω_0, so $(\omega_0 - \omega)$ goes to zero at the resonance condition and the above equations describe the behavior of the magnetization.

7

APPARATUS

Present-day NMR spectrometers frequently use separate coils for excitation and detection of nuclear resonances. These coils are mutually perpendicular to each other as well as to the polarizing field. This perpendicular arrangement insures that no signal will be induced directly in the receiving coil. However, nuclei in the sample which have been excited to an upper spin state emit energy as they fall back to lower levels, and through this mechanism a signal is induced in the receiving coil at resonance.

The idealized perpendicularity of the transmitting and receiving coils is difficult to achieve in practice, and a certain degree of capacitive coupling owing to incomplete orthogonality is actually obtained. To avoid this difficulty, tuning devices are used to steer the flux between the two coils so that direct coupling is eliminated. Two tuning devices are used, one controls the in-phase induced voltage, the other controls the 180-degree out-of-phase induced voltage. A leakage can be induced by detuning either of these tuning devices. The detection of u-mode or v-mode signal in the receiver coil depends on the way these tuning devices are used to produce the leakage.

Quantitatively, the voltage which is induced in the receiver coil along the y-axis, with the transmitter coil along the x-axis and magnetic field along the z-axis, is given by

$$V = - \xi \frac{dM_y}{dt}$$

where ξ is a constant which depends on the sample and on the coil geometry. In terms of the Block susceptibility

$$M_y = 2H_1 (\chi'' \cos \omega t - \chi' \sin \omega t) .$$

This gives

$$V = 2\xi\omega H_1 (\chi'' \sin \omega t + \chi' \cos \omega t) .$$

Thus, the u-mode signal is proportional to $\omega H_1 \chi'$ and the v-mode signal is proportional to $\omega H_1 \chi''$. This means

$$u \propto \frac{\omega \chi_0 H_0 \gamma H_1 T_2^2 (\omega_0 - \omega)}{1 + T_2^2 (\omega_0 - \omega) + \gamma^2 H_1^2 T_1 T_2}$$

and

$$v \propto \frac{\omega \chi_0 H_0 \gamma H_1 T_2}{1 + T_2^2 (\omega_0 - \omega)^2 + \gamma^2 H_1^2 T_1 T_2} .$$

A block diagram of an NMR spectrometer is shown in Figure 1. The magnet is energized by a highly stable dc power supply. If a fixed-frequency r.f. oscillator is used, one sweeps through the resonance by varying the total magnetic field through injection of the linearly varying output from a sweep generator into coils either wound around the magnet pole faces or located within the pole gap.

The H_1 oscillating field is provided by the r.f. current flow through the transmitter coil surrounding the sample. As the dc sweep current is varied and the resonance condition is fulfilled, there is an absorption of power by the sample from the transmitter coil, to initiate transition between its nuclear states and thus induce a voltage in the receiver coil. This induced voltage is phase detected after amplification. Phase detection is used to improve the sensitivity and is accomplished through a low frequency modulation about the resonant field strength, thus causing the resonant nuclei to pass in and out of resonance twice in each cycle.
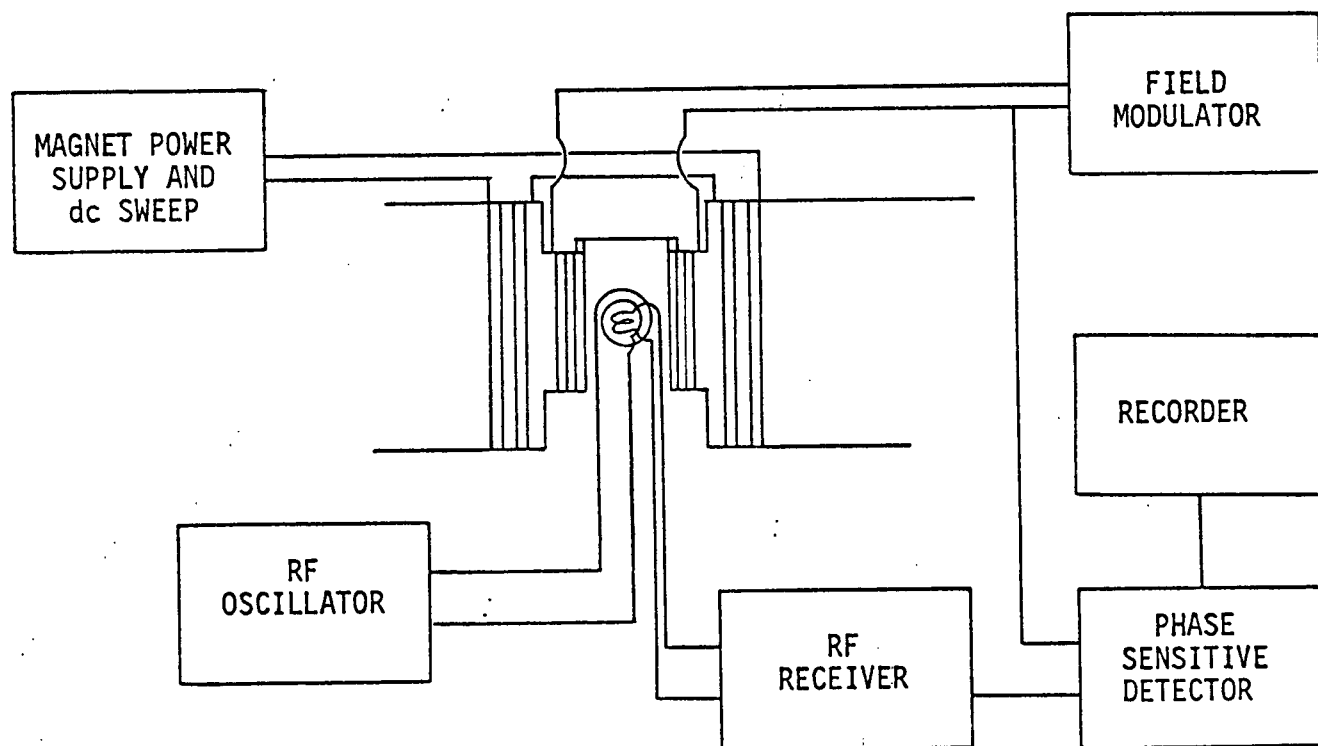
FIGURE 1. BLOCK DIAGRAM OF A NMR SPECTROMETER

PROBLEMS AND LIMITATIONS OF THE NMR SYSTEM

Most of the electrical noise problem initially associated with the NMR system (Fig. 2) were eliminated by providing proper isolation and ground connections. To find the source of the remaining noise and transients, a circuit was designed which will generate the same type of signal as the r.f. unit. This signal was fed to the detection and recording system. This test clearly showed that the detection and recording system was not the cause of the noise and transients (Fig. 3). The transients as seen in Figure 2 were due to some inherent design problem with the r.f. unit. For this reason the r.f. unit had to be sent to the manufacturer.

It was then possible to detect problems associated with the Alpha magnet system. It was felt that the magnetic field might be drifting, indicating an instability associated with the magnet power supply. Resonance spectra of 20 percent D_2O were recorded with a recurrent sweep of 5 minutes, as shown in Figure 4. This clearly demonstrated the drift in the magnetic field. The drift rate was then determined by measuring the actual magnetic field as a function of time with a proton resonance gaussmeter. The drift was found to be linear for the first 20 minutes after turn-on and then decreased monotonically with time. The field was reduced by 20 gauss in about 140 minutes (Fig. 5). The trouble was located within the regulator circuit of the power supply. To reduce the drift in the magnetic field, an additional regulator circuit was built. This reduced the drift problem quite appreciably, but to bring the magnetic field drift within the tolerance demanded by high precession NMR measurement of small concentrations of nuclei, an elaborate regulator circuit has to be designed. The quality of the resonance signal that is obtained after this trouble-shooting is shown in Figure 6.
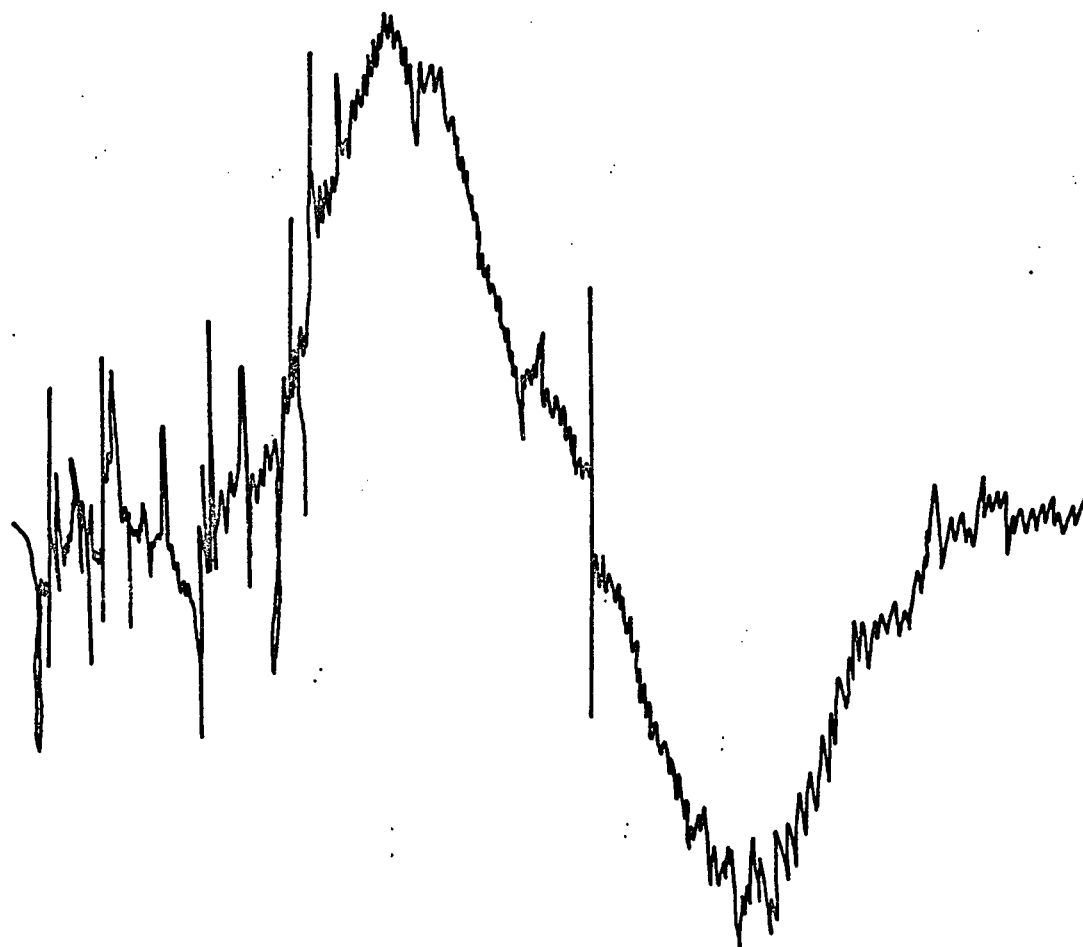
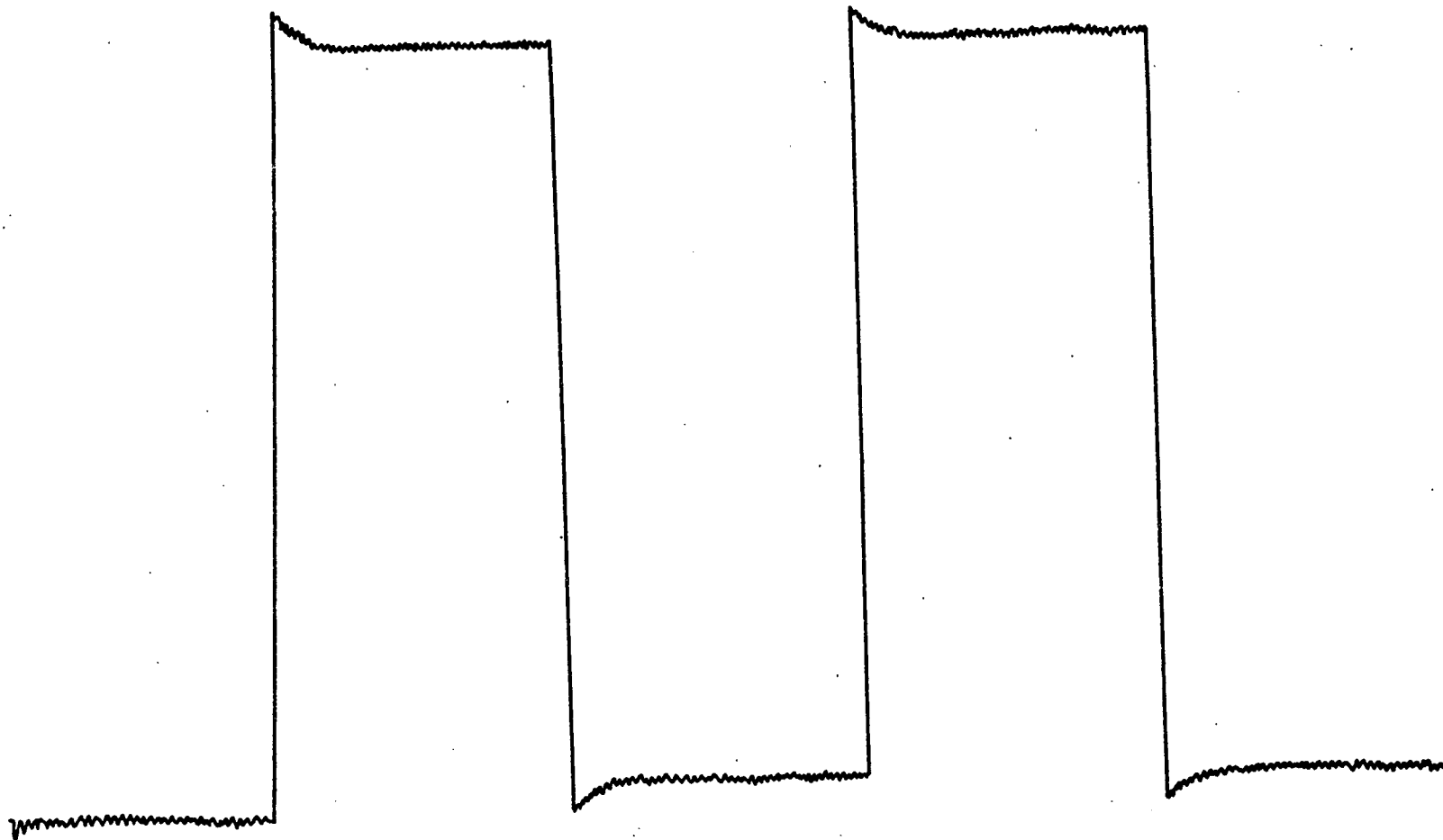FIGURE 2.   RESONANCE OF 20 PERCENT D_2O IN WATER

12

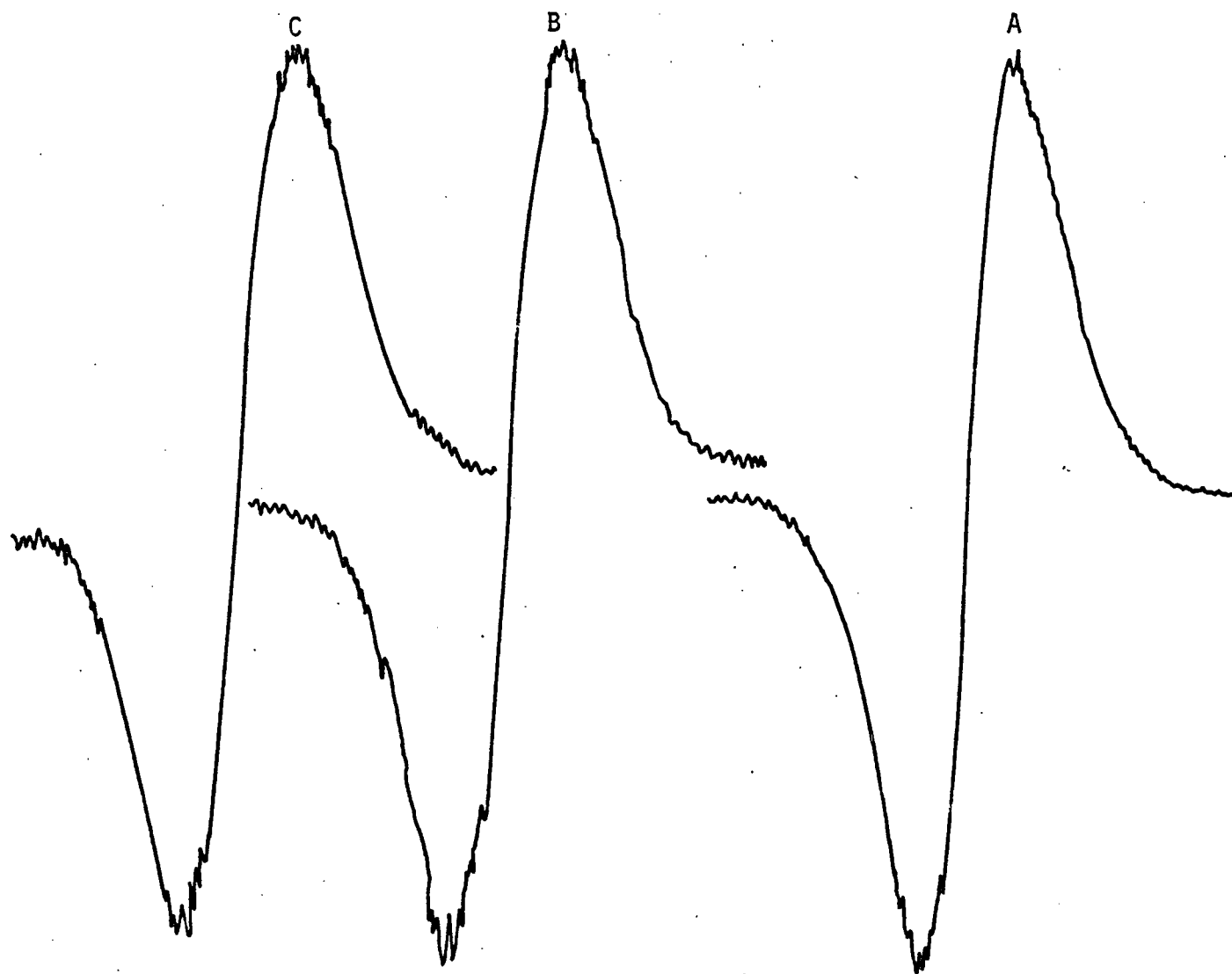FIGURE 3.   NOISE LEVEL OF DETECTION AND RECORDING SYSTEM

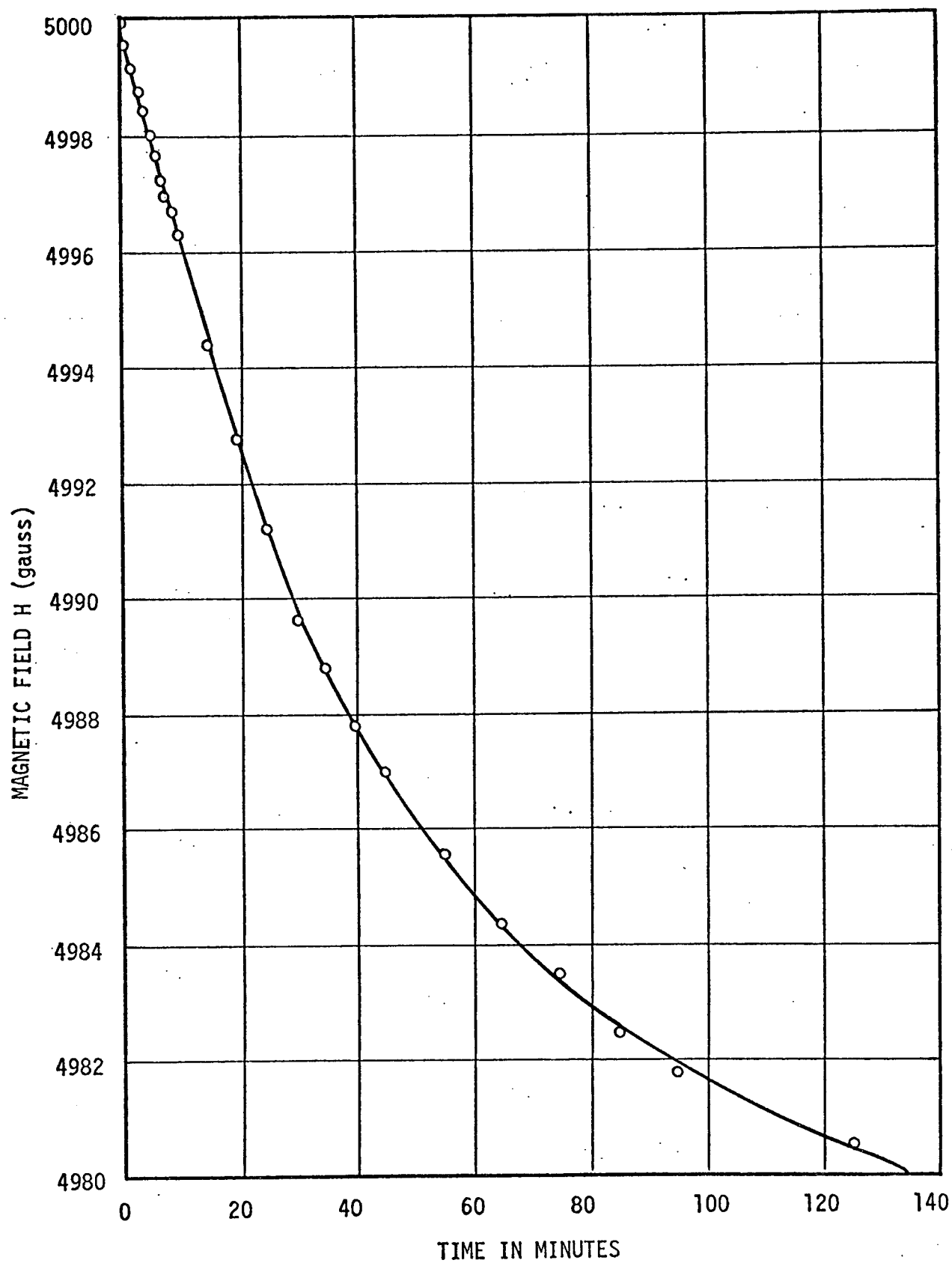FIGURE 4.   RESONANCES OF 20 PERCENT D_2O IN WATER WITH RECURRENT SWEEP OF 5 MINUTES

14

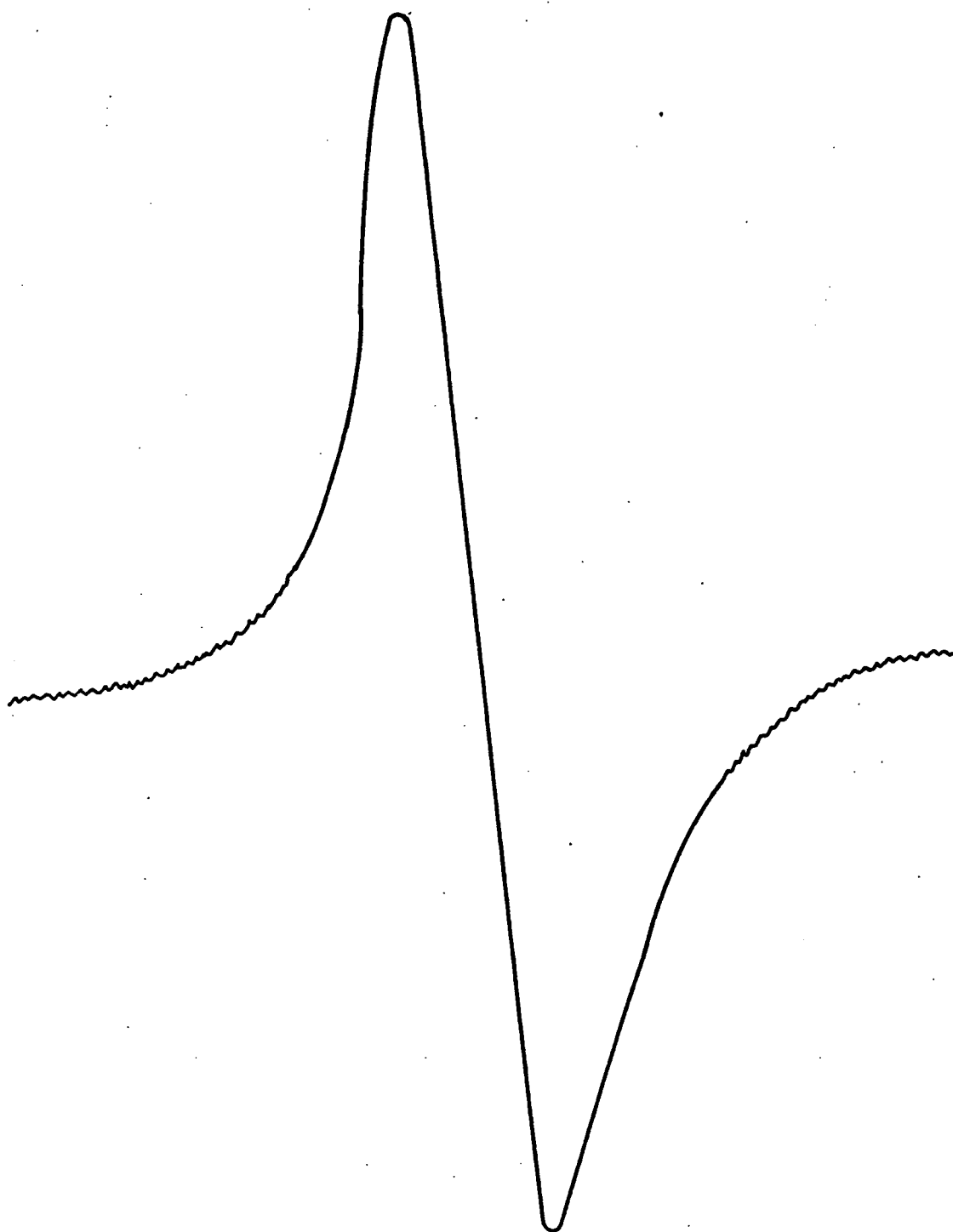FIGURE 5. DRIFT OF MAGNETIC FIELD WITH TIME

15

FIGURE 6.   RESONANCE OF 20 PERCENT D_2O IN WATER

The limitations that exist with the NMR system now are:

- Reducing the magnetic field drift to a stability of 10 mG or better for precise measurement of small concentrations of magnetic nuclei of the order of 10^{22} nuclei per cc

- Addition of a time averaging computer to study the NMR of specimens having magnetic nuclei concentrations of 10^{20} per cc and lower.

CALIBRATION

The system was calibrated using several different materials. Only those materials were chosen for which the field-frequency relation, linewidth and line shape were very well known. The first calibration standard used was a solution of 20 percent D_2O in water. The resonance spectra for D_2 nuclei is shown in Figure 6. This nucleus is supposed to give a resonance signal at a magnetic field of 5.0 kG for a frequency of 3.2678 MHz as calculated from its magnetogyric ratio. The present experiment gives a field value of 5.2032 kG for a frequency of 3.2678 MHz. This difference in the field value is because of the lack of calibration of the Alpha Fieldial system. This difficulty has been overcome by measuring the resonance field precisely with a proton resonance gaussmeter. The measurements were repeated with 2 percent D_2O in water (Fig. 7-a). These measurements were utilized to check the linearity of the output control unit and the homogeneity of the magnetic field within the sample volume. The sensitivity of the system was measured using 0.2 percent D_2O in water. The resonance signal is shown in Figure 7-b. The signal-to-noise ratio was found to be lower than described in the literature. The low signal-to-noise ratio is because of the aforementioned magnetic field instability and drift. This instability and drift is undesirable and precise measurement of
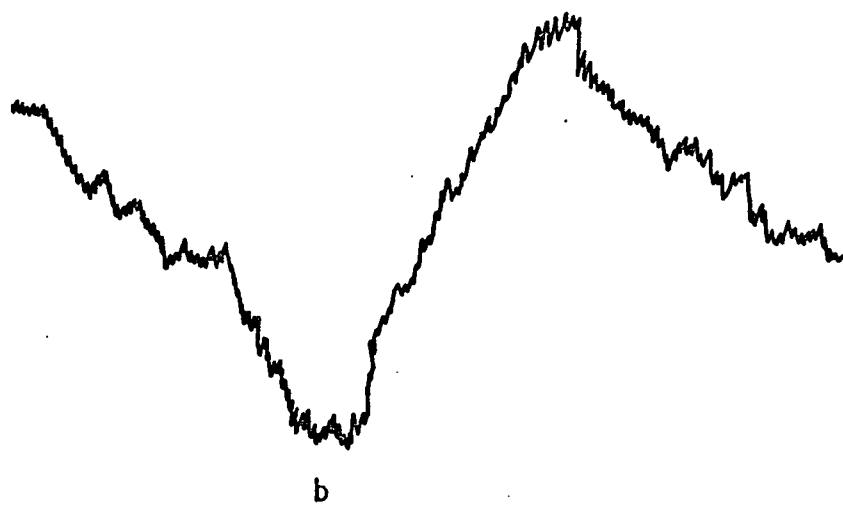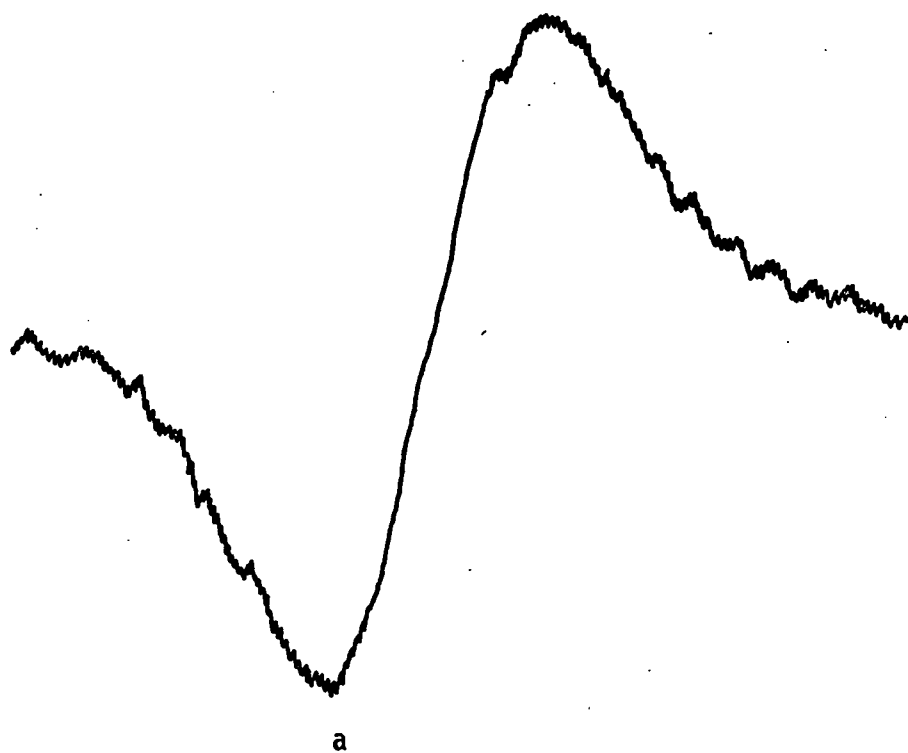
FIGURE 7. RESONANCES OF 2.0 PERCENT AND 0.2 PERCENT D_2O IN WATER

low concentration of magnetic nuclei is practically impossible. The calibration of the system was further checked by locating the proton resonance in methyl and butyl alcohols. The resolution of the instrument was checked by running the NMR spectra of ammonium nitrate solution in water as shown in Figure 8. The separation between the two N^{14} peaks is about 4.75 gauss and demonstrates the adequate resolution of the system.

20

FIGURE 8.   RESONANCE OF N^{14} NUCLEI IN AMMONIUM NITRATE SOLUTION

RESULTS AND DISCUSSION

The results are discussed in two parts. The first part deals with zinc oxide and zinc orthotitanate, and the second part deals with FEP Teflon.
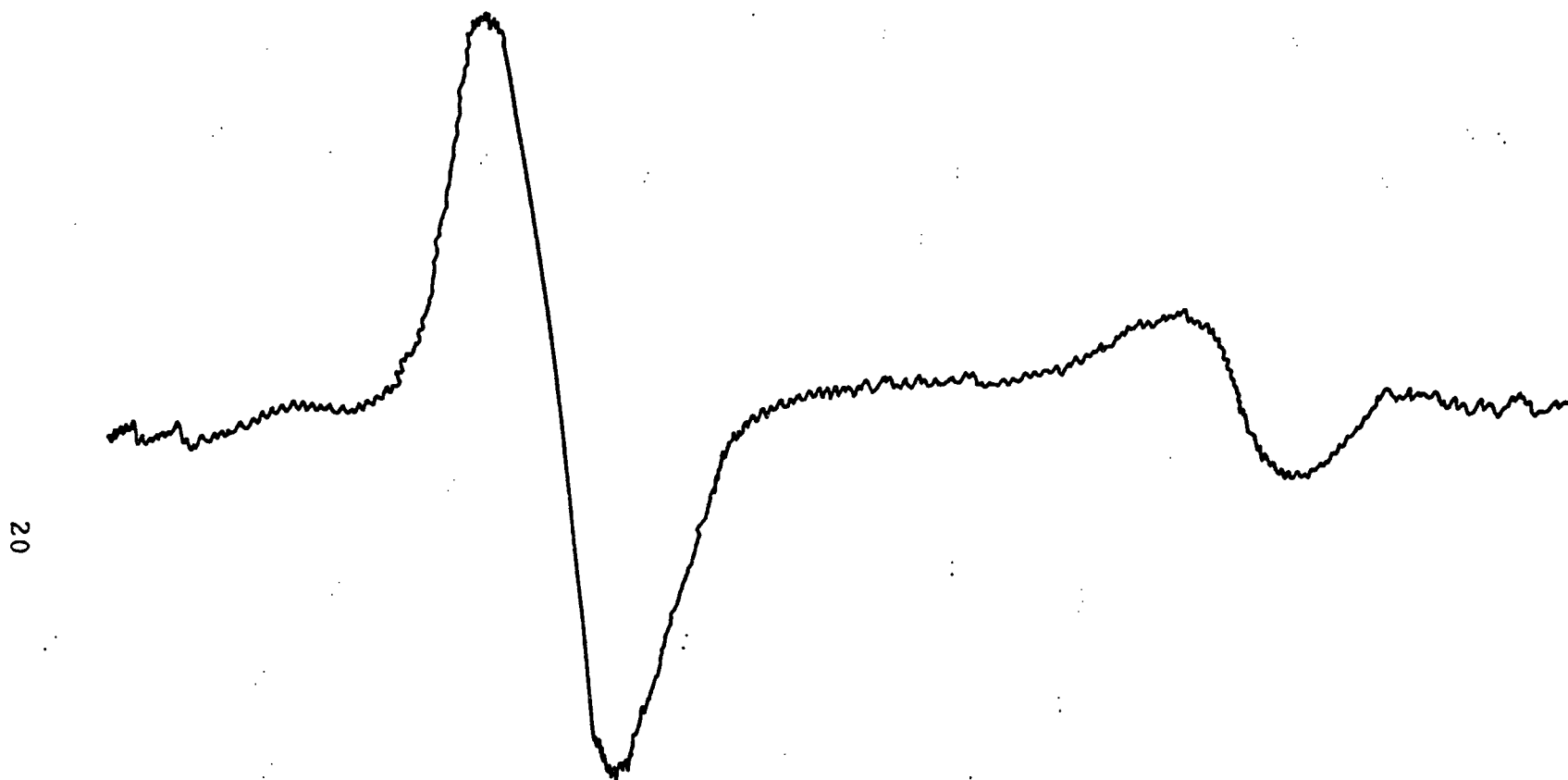
ZnO AND Zn_2TiO_4

Zinc oxide has two nuclei with non-zero magnetic moment, whereas zinc orthotitanate has three nuclei. These nuclei along with their natural abundances, nuclear spins, magnetic moments, and quadrupole moments are shown in Table 1.

TABLE 1.

NUCLEUS	NATURAL ABUNDANCE	SPIN I	MAGNETIC MOMENT (μ)	QUADRUPOLE MOMENT (Q)
Zn^{67}	4.12	5/2	0.8735	0.18
Ti^{47}	7.75	5/2	-0.7871	--
Ti^{49}	5.51	7/2	-1.1022	--
O^{17}	0.037	5/2	-1.893	-4×10^{-3}

As can be seen from Table 1, out of the two probing nuclei in ZnO, one has an appreciable amount of quadrupole moment and the other has a very low natural abundance. The failure to observe Zn^{67} resonance signal in ZnO can be argued theoretically as discussed below.

If the nuclear spin I is equal to or greater than 1, then the interaction of it and the electric quadrupole moment Q with an

21

electrostatic potential V due to changes external to it is given by the Hamiltonian (Ref. 4)

$$\mathcal{H} = [eQ/4I(2I-1)] [(3I_z^2 - I^2) V_0 + (I_+I_z + I_zI_+) V_{-1}$$

$$+ (I_-I_z + I_zI_-) V_{+1} + I_+^2 V_{-z} + I_-^2 V_{+2})]$$

where $I_{\pm} = I_x \pm iI_y$, $V_0 = V_{zz}$, $V_{\pm 1} = V_{xz} \pm iV_{yz}$, $V_{\pm 2} = \frac{1}{2}(V_{xx} - V_{yy})$ $\pm iV_{xy}$ and where $V_{xy} = \partial^2 V/\partial x \partial y$, etc. The z-axis can be taken along the direction of the external magnetic field H.

Now if V at the position of a nucleus has cubic symmetry, then the quadrupole interaction vanishes, and the resonance line consists of one line at the nuclear Larmar frequency ω_0 and of a width solely determined by magnetic dipole-dipole interactions between all the nuclei.

This is not the case with ZnO since this material has a hexagonal symmetry; hence, the interaction of the spin I and the quadrupole moment Q, which is appreciable, with the electrostatic potential will be considerable. The quadrupole interaction can be considered as a perturbation on the (2I + 1) energy levels in the magnetic field H_0. Introducing the quantity

$$eq = \sum_j e_j (3 \cos^2 \phi_j - 1) r^{-3}$$

where ϕ_j is the angle between the radius vector r_j towards a charge e_j in the lattice and the axis of symmetry at the origin; and denoting the angle between this symmetry axis and the magnetic field by θ, the

energy difference between the levels m_I and $m_{(I-1)}$ is given by

$$\Delta E_{m \to (m-1)} = h\nu_0 + (2m - 1)(3\cos^2\theta - 1)\frac{3e^2qQ}{8I(2I-1)} \cdot$$

As can be seen from this equation, the central transition is unperturbed. For larger quadrupole interaction, the second order perturbation theory gives

$$\Delta E = h\nu_0 \frac{9}{64} \frac{2I+3}{4I^2(2I-1)} \frac{e^4Q^2q^2}{h\nu_0}(1 - 9\cos^2\theta)(1 - \cos^2\theta)$$

for the transition between the levels $m_I = \frac{1}{2}$ and $-\frac{1}{2}$. In polycrystalline non-cubic crystals the resonance of the satellite lines will be spread over a large frequency interval, as $(3\cos^2\theta - 1)$ ranges from its maximum value of 2 to its minimum value of -1. In second order effect even the central component will be broadened.

It is thus possible that due to the strong quadrupole interaction the Zn^{67} resonance line in ZnO is so broadened that it is no longer detectable. The same argument applies for the Zn^{67} resonance in Zn_2TiO_4.

An attempt to detect the O^{17} resonance line in ZnO was also unsuccessful. The reason may be twofold: The first is the broadening of the resonance due to the interaction of the electric quadrupole moment of the O^{17} nucleus with the electric field gradient at the oxygen site in the lattice. The second reason is probably the drift and fluctuation of the magnetic field, a limitation with the present system, as mentioned before. Because of this limitation, resonance signal using 0.02 percent

D_2 in water could not be obtained, though this amount of D_2 (half the amount of O^{17} abundance) should give a resonance signal with signal-to-noise ratio of about 10. Thus it is strongly felt that the limitation with the magnet system is responsible for the failure. The same argument applies to Zn_2TiO_4. Moreover, only a very minute quantity of Zn_2TiO_4 could be obtained through personal contact and it is not available commercially.

It is believed that O^{17} resonance in both the materials can be observed by using a time-averaging computer, as mentioned before, and using materials artificially enriched with O^{17} nuclei.

FEP TEFLON

This material is a copolymer of tetrafluoroethylene and hexa-fluoropylene and should give magnetic resonance due to F^{19} nuclei. The natural abundance of this nuclei is 100 percent. The F^{19} nucleus has a spin of $\frac{1}{2}$ and magnetic moment 2.627.

The F^{19} resonance in FEP Teflon is shown in Figure 9. The small hump in the resonance signal probably shows that the material under investigation has two forms, one crystalline and the other amorphous. The F^{19} resonance in this material has a line width of about 5.2 gauss and compares favorably with the data quoted in the literature (Ref. 5).

For a resonance curve described by a normalized shape function $f(\omega)$ with a maximum at a frequency ω_0, the nth moment M_n with respect to the point ω_0 is defined as

$$M_n = \int (\omega - \omega_0)^n \, f(\omega) \, d\omega .$$

FIGURE 9. F^{19} RESONANCE IN FEP TEFLON

If $f(\omega)$ is symmetrical with respect to ω_0, all odd moments vanish. For a Gaussian curve the normalized shape function in terms of magnetic field H is

$$\xi(H) = \frac{A}{\sqrt{2}\ \pi\ \Delta H_2}\ \exp\left[\frac{-\ (H-H_0)^2}{2\Delta H_2^2}\right]$$

so that $\xi_{max} = A/\sqrt{2}\ \pi\ \Delta H_2$. H_0 is the center of the curve which is, usually, symmetric and ΔH_2 is the second moment; the mth power of the mth moment is thus given by

$$\Delta H_m^m = \frac{\int \xi\ (H)\ (H-H_0)^m\ d\ (H-H_0)}{\int \xi\ (H)\ d\ (H-H_0)}\ ,$$

The experimental second moment ΔH_2 for the F^{19} resonance in FEP Teflon is about 1.5 gauss^2, as compared to the theoretical rotating chain second moment of 0.9 gauss^2.

Short time ultraviolet irradiation of FEP Teflon showed no detectable change in F^{19} resonance signal. It is possible that such short term irradiation is unable to bring about chain scission and production of monomers.

RECOMMENDATIONS

As mentioned before, the stability of the magnetic field should be improved by incorporating within the power supply system a better regulator circuit. Without this it is not possible to increase the sensitivity of the NMR system to the point that it can detect the 0.02 percent D_2 resonance with a signal-to-noise ratio of 10. Without a sensitivity level this great it is practically impossible to detect the resonance of materials with low natural abundance.

It is also suggested that a time-averaging computer be added to the NMR system. With the help of this computer the resonance signal from materials with very low natural abundance can be detected. This will also help in obtaining O^{17} resonance in ZnO and Zn_2TiO_4 with adequate signal-to-noise ratio.

The addition of a regulator circuit and time-averaging computer will definitely increase the sensitivity of the system to the level that it will be possible to conduct systemetic investigation of irradiation effects on ZnO and Zn_2TiO_4 thermal control coatings. It is suggested that O^{17} enriched materials be used.

REFERENCES

1. Greenberg, S.A., H. G. MacMillan and A. F. Sklensky, Final Report, NASA Contract NAS8-18114, February 1968

2. Hayes, J. D., et. al., Teledyne Brown Engineering Interim Report RL-INT-632, April 1969

3. Mookherji, T., Teledyne Brown Engineering Interim Report SMSD-SSL-823, August 1969

4. Pound, R. V., Phys. Rev. $\underline{79}$, 685, 1950

5. Hyndman, D. and G. F. Origlio, J. Appl. Phys. $\underline{31}$, 1849, 1960.